Medical Microbiology and Immunology (2023) 212:391–405
https://doi.org/10.1007/s00430-023-00780-x

ORIGINAL INVESTIGATION

CD146 deficiency promotes inflammatory type 2 responses in pulmonary cryptococcosis

Zhengxia Wang[1] · Wei Liu[2] · Huidi Hu[3] · Jingxian Jiang[1] · Chen Yang[3] · Xijie Zhang[1] · Qi Yuan[1] · Xiaofan Yang[4] · Mao Huang[1] · Yanming Bao[5] · Ningfei Ji[1] · Mingshun Zhang[3]

Received: 17 February 2023 / Accepted: 18 August 2023 / Published online: 31 August 2023

Abstract

Cryptococcus neoformans (*C. neoformans*) is an important opportunistic fungal pathogen for pulmonary cryptococcosis. Previously, we demonstrated that CD146 mediated the adhesion of *C. neoformans* to the airway epithelium. CD146 is more than an adhesion molecule. In the present study, we aimed to explore the roles of CD146 in the inflammatory response in pulmonary cryptococcosis. CD146 was decreased in lung tissues from patients with pulmonary cryptococcosis. Similarly, *C. neoformans* reduced pulmonary CD146 expression in mice following intratracheal inoculation. To explore the pathological roles of CD146 reduction in pulmonary cryptococcosis, CD146 knockout (KO) mice were inoculated with *C. neoformans* via intratracheal instillation. CD146 deficiency aggravated *C. neoformans* infection, as evidenced by a shortened survival time and increased fungal burdens in the lung. Inflammatory type 2 cytokines (IL-4, IL-5, and TNF-α) and alternatively activated macrophages were increased in the pulmonary tissues of CD146 KO-infected mice. CD146 is expressed in immune cells (macrophages, etc.) and nonimmune cells, i.e., epithelial cells and endothelial cells. Bone marrow chimeric mice were established and infected with *C. neoformans*. CD146 deficiency in immune cells but not in nonimmune cells increased fungal burdens in the lung. Mechanistically, upon *C. neoformans* challenge, CD146 KO macrophages produced more neutrophil chemokine KC and inflammatory cytokine TNF-α. Meanwhile, CD146 KO macrophages decreased the fungicidity and production of reactive oxygen species. Collectively, *C. neoformans* infection decreased CD146 in pulmonary tissues, leading to inflammatory type 2 responses, while CD146 deficiency worsened pulmonary cryptococcosis.

Keywords *Cryptococcus neoformans* · Lung infection · CD146 · Macrophages · Inflammation · Bone marrow chimera

Introduction

Cryptococcus neoformans (*C. neoformans*) is an important, opportunistic fungal pathogen for invasive pulmonary mycosis [1]. Once inhaled into respiratory tracts, *C. neoformans*

Edited by Christian Bogdan.

Zhengxia Wang, Wei Liu and Huidi Hu contributed equally to the work.

✉ Yanming Bao
bymszchildren@email.szu.edu.cn

✉ Ningfei Ji
jnf@njmu.edu.cn

✉ Mingshun Zhang
mingshunzhang@njmu.edu.cn

[1] Department of Respiratory and Critical Care Medicine, The First Affiliated Hospital of Nanjing Medical University, Nanjing 210029, China

[2] NHC Key Laboratory of Antibody Technique, Jiangsu Province Engineering Research Center of Antibody Drug, Jiangsu Key Laboratory of Pathogen Biology, Department of Immunology, Nanjing Medical University, Nanjing 211166, Jiangsu, China

[3] Department of Pathology, Nanjing Chest Hospital, The Affiliated Brain Hospital of Nanjing Medical University, Nanjing 210029, China

[4] The Laboratory Center for Basic Medical Sciences, Nanjing Medical University, Nanjing 211166, Jiangsu, China

[5] Department of Respirology, Shenzhen Children's Hospital, Shenzhen 518026, Guangdong, China

may deeply penetrate into pulmonary alveoli. To establish infection in pulmonary alveoli, *C. neoformans* must survive against diverse immune cells, i.e., macrophages and neutrophils. Resident alveolar macrophages, infiltrated macrophages, and neutrophils constitute the first line of immune defenses. Classically activated macrophages (M1) favor the clearance of *C. neoformans;* in contrast, alternatively activated macrophages (M2) are permissive to the proliferation and dissemination of *C. neoformans* [2]. Similarly, neutrophils perform multiple tasks in pulmonary cryptococcosis [3]. Neutrophils not only directly kill *C. neoformans* [4] but also modulate the immune responses and even, paradoxically, increase susceptibility to pulmonary cryptococcosis [5]. Macrophages and neutrophils play critical roles in the early stage of *C. neoformans* pulmonary infection.

CD146, originally identified as a melanoma cell adhesion molecule (MCAM), is widely distributed in different tissues and cells. Previously, we demonstrated that CD146 in epithelial cells mediated the adhesion of *C. neoformans* to respiratory tracts [6]. However, CD146 is more than an adhesion molecule [7]. CD146 is expressed by various immune cells, i.e., macrophages and neutrophils. In vitro, CD146 promotes monocyte migration [8]. In vivo, the evidence of CD146 in the activation and migration of macrophages in the model of atherosclerosis is being debated [9, 10]. In adipose tissues, CD146 in macrophages promotes the polarization of M1 macrophages [11]. In addition to macrophages, CD146 in neutrophils is involved in the pathogenesis of active small-vessel vasculitis [12]. CD146 regulates the activation and polarization of macrophages and neutrophils.

Previously, we demonstrated that CD146 deficiency decreased the adhesion of *C. neoformans* to epithelial cells and reduced the fungal burden in a 4-h acute infection model [13]. In the present study, we aimed to explore the roles and potential mechanisms of CD146 in the inflammatory response to pulmonary cryptococcosis. To investigate whether CD146 was involved in *C. neoformans* pulmonary infection, we examined the expression of CD146 in clinical samples with pulmonary cryptococcosis and mouse lung tissues with pulmonary infection. To dissect the mechanisms of CD146 regulation in pulmonary cryptococcosis, we compared pulmonary infections in wild-type (WT), CD146 knockout (KO), and bone marrow chimeric mice. Furthermore, CD146 KO macrophages and neutrophils were analyzed for their potential to kill fungi.

Materials and methods

Study population and pulmonary tissues

Lung tissue biopsies from 10 immunocompetent patients diagnosed with pulmonary cryptococcus nodules were obtained from Nanjing Chest Hospital (Table 1). Healthy tissues were defined as tissues at least 5 cm from the cryptococcus nodules. Patients with HIV-1 infection, tuberculosis, diabetes, transplantation, hepatocirrhosis, cancer, or any other known risk factors that weakened immune responses were excluded. The ethical review was approved by the Nanjing Chest Hospital ethics committee.

Mice

Six- to eight-week-old female C57BL/6J mice were purchased from the Laboratory Animal Center, Nanjing Medical University (Nanjing, China). $CD146^{-/-}$ (CD146-KO) mice generated with CRISPR/Cas9 techniques on the C57BL/6J background were obtained from Cyagen (Suzhou, China). In brief, gRNA to mouse *CD146* exons 2–9 and Cas9 mRNA were co-injected into fertilized mouse eggs to generate targeted knockout offspring. Homozygous CD146 KO mice were generated by intercrossing heterozygous F1 mice. All mice were maintained under specific-pathogen-free (SPF) conditions at the Animal Core Facility of Nanjing Medical University. All animal treatments were in accordance with the guidelines approved by the Institutional Animal Care and Use Committee of Nanjing Medical University (*IACUC-1708004*).

Culture and maintenance of C. neoformans

C. neoformans type strain H99 (ATCC, 208821) maintained in liquid nitrogen in 25% glycerol was expanded in Sabouraud dextrose medium (Becton Dickinson, 238230) overnight in a rotating incubator at 30 ℃. They were washed three times with sterile phosphate-buffered saline (PBS) and counted in a hemocytometer. Subsequently, fungi were resuspended to a desired concentration in normal saline (NS) for in vivo infection or in PBS for in vitro stimulation. In

Table 1 Clinical characteristics of 10 patients with pulmonary cryptococcosis

No	Sex	Age (year)	Chest CT/disease
1	Male	55	Nodules of the lower right lung
2	Female	61	Nodules of the right upper lung
3	Male	67	Nodules of the lower right lung
4	Female	49	Nodules of the lower right lung
5	Male	52	Nodules of the lower right lung
6	Male	28	Nodules of the lower left lung
7	Female	56	Nodules of the upper left lung
8	Female	41	Nodules of the lower right lung
9	Female	49	Nodules of the lower left lung
10	Male	55	Nodules of the upper left lung

some experiments, fungi were heat-killed by incubation in a 60 °C water bath for 1 h [14].

Intratracheal infection with C. neoformans

For intratracheal instillation of *C. neoformans*, mice were anesthetized i.p. with pentobarbital sodium. Then, 1×10^4 H99 cells in 30 µl NS were injected into the airway by using a 1 ml syringe and a 30-gauge needle, which was followed quickly by 200 µl air to help H99 diffuse in airways [15]. Mice were monitored daily for survival following surgery.

In some experiments, 1×10^4 heat-killed H99 cells were injected into the airway, and the mice were sacrificed 2 weeks post infection.

CFU analysis

Wild-type and $CD146^{-/-}$ mice infected with H99, as described above, were euthanized, and the lungs, spleens, and brains were excised for CFU analysis at the indicated time points to determine fungal burden and dissemination. Briefly, the organs were homogenized in 1 ml of PBS using a tissue homogenizer. In addition, various dilutions of the homogenized tissues were plated on Sabouraud dextrose agar (Becton Dickinson, 210950), and the colonies were counted following incubation at 32 °C for 48 h.

Histopathological analysis

The lung specimens obtained from mice at the indicated time points were fixed in 4% paraformaldehyde, dehydrated, and embedded in paraffin. Sections were cut into 7 µm slides and stained with hematoxylin and eosin (H&E) or periodic acid–Schiff (PAS) using standard staining procedures at the pathology platform of Servicebio Technology, Wuhan, China. Images of the slides were acquired with an Olympus BX51 light microscope (Olympus Canada) at a magnification of 400×.

Immunohistochemistry and immunofluorescence imaging

Formaldehyde-fixed mouse lungs were dehydrated, paraffin-embedded, and sectioned (5 µm thickness). Sections were rehydrated, quenched with 3% hydrogen peroxide, incubated in citric buffer for antigen retrieval, and blocked with the avidin/biotin blocking system and then 5% normal goat serum, followed by overnight incubation at 4 ℃ with primary anti-CD146 antibody (ab75769, Abcam, 1:500) or with PBS as blank controls (Figure S5). Tissue sections were then incubated with horseradish peroxidase-conjugated secondary antibodies for 1 h at room temperature. The staining was visualized with 3,3′-diaminobenzidine (DAB, Vectastain, Vector Laboratories, USA) and background–stained with hematoxylin. All CD146-stained sections were scanned with a Zeiss Axio Examiner microscope, and representative photos were chosen and presented for each stimulus group in the study. $CD146^+$ cells on the tissue slide were quantified by a customized cellular multiplex algorithm using Halo v3.0.311.314 [16].

For the clinical lung tissues, immunohistochemistry was performed with an automated immunohistochemistry staining system (Ventana BenchMark ULTRA, Ventana Medical Systems) using the 3,3′diaminobenzidine method. In brief, following deparaffinization and heat-induced antigen retrieval for 60 min, the tissue sections were incubated for 30 min at 37 °C with anti-CD146 antibody (ab75769, Abcam, 1:500) or as PBS blank controls (Fig. 1A). A subsequent amplification step was followed by incubation with hematoxylin II counter stain for 8 min and then a blue-coloring reagent for 8 min according to the manufacturer's instructions (Ventana). For immunofluorescence, slides were then fixed with 4% paraformaldehyde, rinsed twice with PBS, and permeabilized in PBS 0.5% Triton X-100. Samples were incubated with 5% normal goat serum for 1 h at room temperature (RT) and stained in blocking buffer with anti-CD146 (ab75769, Abcam, 1:3000) overnight at 4 °C. After the samples were washed with PBS, secondary antibodies conjugated with horseradish peroxidase (HRP) were added to the samples and incubated for 1 h in the dark at RT. Tyramide signal amplification (CY3-TSA) was used to amplify the fluorescence. The samples were finally mounted with DAPI (Yeasen, 36308). Images of the slides were captured by a ZEISS LSM710 confocal laser scanning microscope.

Bronchoalveolar lavage fluid (BALF) harvest

At the designated time points, the tracheae of the mice were exposed, and BALF was collected by lavage with ice-cold PBS (500 µl × 3; 85%– 90% of the lavage volume was recovered) via a tracheal catheter. BALF from each mouse was centrifuged at 1000 rpm for 10 min at 4 °C, and the total number of inflammatory cells in BALF was examined by flow cytometry analysis. The supernatant of BALF was collected and frozen at − 80 °C for enzyme-linked immunosorbent assay (ELISA).

Flow cytometry for cell counting

The cell pellet was counted in a hemocytometer. BALF cells were washed twice with protein-free PBS and incubated with a Zombie NIR™ Fixable Viability Kit (423105, Biolegend) at room temperature for 30 min in the dark. After washing twice with 1% bovine serum albumin (BSA), the cells were stained with a CD16/CD32 FcR blocking antibody (14-0161-85, eBioscience)

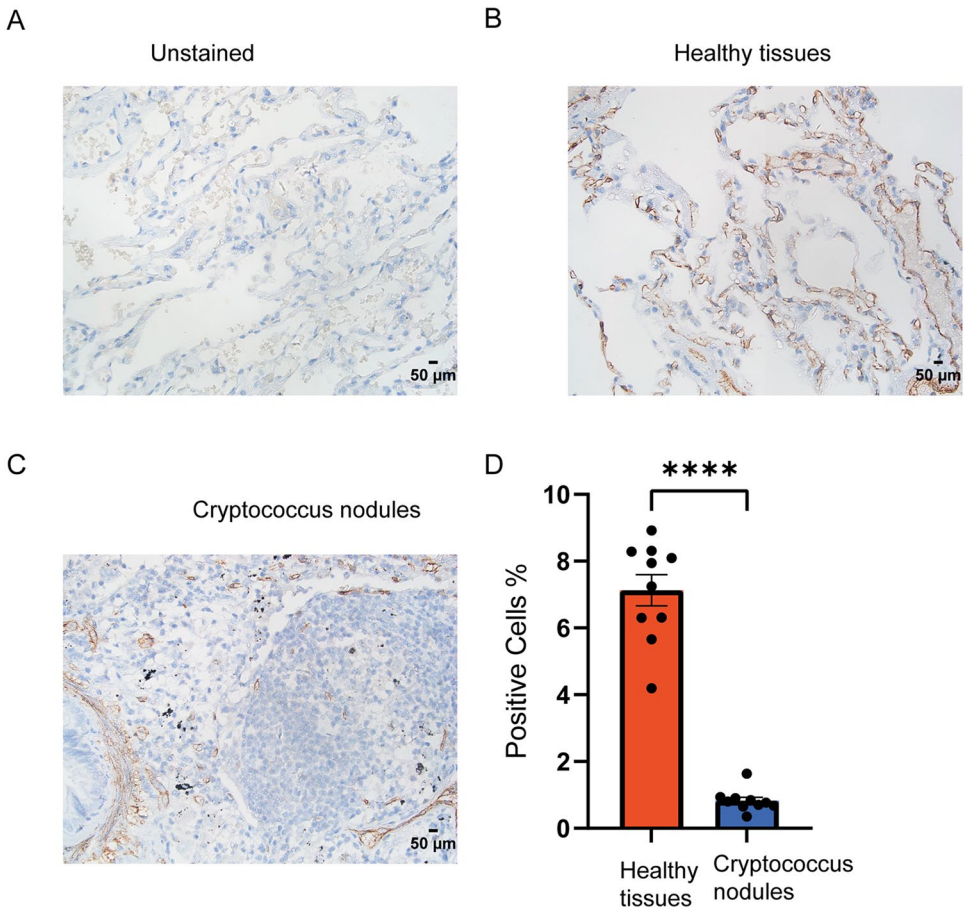

Fig. 1 CD146 was decreased in patients with *C. neoformans* pulmonary infection. **A**–**C** Immunohistochemical staining for CD146 in lung sections, **A** was for negative control, **B** was for healthy tissues 5 cm distance from the nodules, and **C** was for cryptococcus nodules (n = 10). **D** The quantitative analysis of CD146 in lung section ****, $p < 0.0001$

for 10 min. Then, the cells were fixed and permeabilized (554714, BD Biosciences) in accordance with the instructions of the manufacturer. Subsequently, the BALF cells were incubated with anti-CD45-PE-cy7 (1103114, Biolegend), anti-CD11b-BV510 (101245, Biolegend), anti-Ly6G-Alexa Fluor647 (127610, Biolegend), and anti-F4/80-Alexa Fluor488 (53-4801-82, eBioscience) in the dark at 4 °C for 1 h, in accordance with the instructions of the manufacturer. Neutrophils were recognized as $CD45^+Ly6G^+CD11b^+$, and macrophages were recognized as $CD45^+F4/80^+$ (Figure S1). Data were acquired with a FACSVerse (BD Biosciences) and analyzed using FlowJo software (Treestar, Woodburn, OR, USA).

Enzyme-linked immunosorbent assay (ELISA)

The levels of IL-4, IL-5, IFN-γ (431104, 431204, 430804, Biolegend), KC, MCP-1 (DY453, DY479, R&D), and TNF-α (88-7324-88, Invitrogen) in BALF, lung homogenates, and cell supernatants were measured using commercial ELISA kits in accordance with the manufacturer's instructions.

Quantitative real-time PCR

Total RNA was extracted from fresh lung tissue or cells with a TRIzol reagent kit (Life Technologies) in accordance with the manufacturer's instructions. The mRNAs were reverse-transcribed with cDNA synthesis supermix for qPCR (11141, Yeasen). Quantitative real-time PCR (qRT−PCR) was performed with a StepOnePlus Real-Time PCR System (ABI, USA). Each reaction well contained 5 μl Universal Blue SYBR Master Mix (11184, Yeasen), 3 μl RNase-free water, 0.5 μl primers, and 1 μl template. We used the fold change ($2^{-\Delta\Delta CT}$) to show the expression of mRNA. The primers used are shown in Table 2.

Western blot analysis

Total cell or tissue protein was lysed in RIPA buffer (89900, Pierce) with PMSF (ST506, Beyotime Biotech) on ice and centrifuged for 10 min at 12,000 rpm at 4 °C. The supernatant was then transferred to a new tube and denatured in sodium dodecyl sulfate−polyacrylamide gel electrophoresis (SDS−PAGE) loading buffer (20315, Yeasen) with heating at 100 °C for 10 min. The

Table 2 Primers in the study

Name	Sequence
β-Actin-F	GAGAAGCTGTGCTATGTTGCT
β-Actin-R	CTCCAGGGAGGAAGAGGATG
iNOS-F	GTTCTCAGCCCAACAATACAAGA
iNOS-R	GTGGACGGGTCGATGTCAC
Arg1-F	CTCCAAGCCAAAGTCCTTAGAG
Arg1-R	AGGAGCTGTCATTAGGGACATC
CD146-F	GGAAAATCAGTATCTGCCTCTCC
CD146-R	GGAAAATCAGTATCTGCCTCTCC
IL-4-F	GGTCTCAACCCCCAGCTAGT
IL-4R	GCCGATGATCTCTCTCAAGTGAT
IL-5-F	CTCTGTTGACAAGCAATGAGACG
IL-5R	TCTTCAGTATGTCTAGCCCCTG
IL-13-F	CCTGGCTCTTGCTTGCCTT
IL-13-R	GGTCTTGTGTGATGTTGCTCA
IFN-g-F	ACAATGAACGCTACACACTGC
IFN-g-R	CTTCCACATCTATGCCACTTGAG
TNF-α-F	GGAACACGTCGTGGGATAATG
TNF-α-R	GGCAGACTTTGGATGCTTCTT
IL-17A-F	TCAGCGTGTCCAAACACTGAG
IL-17A-R	CGCCAAGGGAGTTAAAGACTTGACTT

supernatant was then stored at − 80 °C. The proteins were separated by 10% SDS−PAGE and transferred at 300 mA for 2 h at 4 °C. The blots were then blocked with 5% non-fat dry milk in TBST and incubated with 1:1000 primary antibodies against β-actin (4970L, Cell Signaling Technology) and CD146 (ab75769, Abcam) overnight before adding HRP-linked anti-rabbit IgG (7074, Cell Signaling Technology, 1:5000). After the membranes were treated with Immobilon Western Chemiluminescent HRP Substrate (WBKLS0500, Merck Millipore, USA), the binding of specific antibodies was visualized using a Syngene G: BOX Imaging System and analyzed with ImageJ.

Isolation of alveolar macrophages

The C57BL/6J mice were sacrificed for collection of alveolar macrophages. The lungs of each mouse were lavaged eight times using 1 ml PBS to isolate alveolar macrophages, as previously described [17]. Briefly, cells were collected by low-speed centrifugation and washed twice in complete RPMI 1640 medium. Cells were allowed to adhere for 6 h in a 96- or 24-well plate. After washing with PBS, the adherent cells were alveolar macrophages, as identified by flow cytometry [18].

Bone marrow-derived macrophage (BMDM) culture

Tibias and femurs were excised, and marrow cells were flushed, lysed with Red Blood Cell Lysis Buffer, and resuspended at $3*10^5$ cells/ml in Dulbecco's minimal essential medium (DMEM) containing 10% fetal calf serum, penicillin, streptomycin, and 20 ng/ml recombinant mouse GM-CSF (576308, Biolegend) [19]. The medium was changed every 3 days. After 7 days, the resultant nonadherent cell populations were discarded, and the remaining adherent cells (BMDMs) were collected for further use. The efficiency of differentiation was validated using flow cytometry (Figure S3).

In Vitro *killing assay*

C. neoformans strain H99 was opsonized in 10% normal mouse serum at 37 °C for 45 min. Alveolar macrophages or BMDMs were seeded in a 96-well culture plate and infected with normal mouse serum-opsonized *C. neoformans* strain H99 at a multiplicity of infection of 0.02, with H99 in DMEM complete medium without cells as a control. After 24 h, the content of each well was centrifuged, and the supernatants were removed [20]. The pellet was liberated by lysing the macrophages in sterile water. The number of C. neoformans CFUs was determined by plating tenfold serial dilutions for each sample onto Sabouraud dextrose agar plates after 48 h incubation at 30 ℃. The percentage of inhibition was calculated by dividing the CFU for each well by the average CFU in wells without macrophages and then subtracting this from 1 [2, 21].

In Vitro macrophage stimulation

For stimulation with *C. neoformans*, macrophages (AM or BMDM) were plated in 24-well culture plates infected with H99 for 24 h [19], and then supernatants were collected for the detection of KC and TNF-α.

Determination of reactive oxygen species

A reactive oxygen species (ROS) assay kit (S0033, Beyotime) was used to determine ROS in macrophages. BMDMs were plated in a 24-well culture plate infected with H99 for 24 h, and then the cells were incubated with DCFH-DA (diluted 1:1000) in a 37 °C incubator in the dark for 1 h. After washing with DMEM without FBS 3 times, the fluorescence of the cells was visualized with a Zeiss Axio Examiner microscope. To quantitatively analyze the intracellular ROS, we used a microplate reader (Biotek-synergy, USA) to measure the fluorescence intensity of DCFH and set the excitation wavelength to 485 nm and emission wavelength to 528 nm.

Bone marrow chimeras

Six-week-old recipient mice were provided 0.2% neomycin sulfate (60207ES25, Yeasen) in their drinking water for the first 2 weeks before being lethally irradiated by X-ray (5 Gy × 2). Recipient mice were intravenously transferred with 1×10^7 bone marrow leukocytes from the indicated donors. Bone marrow cells from CD146 KO mice were transferred into WT mice (chimeric; CD146 expressed only on nonhematopoietic cells). In contrast, bone marrow cells from the WT mice were transferred into the CD146 KO mice (chimeric; CD146 positive only in the hematopoietic cells). AM originate from the fetal liver and renew in the lung and do not originate from the bone marrow, so these cells still have CD146 or not, depending on the chimera. Irradiated mice were treated for 2 weeks with 0.2% neomycin sulfate. After 8 weeks of hematopoietic reconstitution, mice were intratracheally infected with 1×10^4 *C. neoformans* strain H99.

Statistical analysis

Data were subjected to testing for normal distribution All data are expressed as the mean ± SEM, and all statistical analyses were performed using GraphPad Prism 7. Single comparisons were conducted by unpaired t tests. Multiple comparisons were tested by using one-way ANOVA with Tukey's adjustment. Survival study comparison was performed using Kaplan–Meier analysis. For all analyses, statistical significance was set as *, $P < 0.05$; **, $P < 0.05$; ***, $P < 0.01$; ****, $P < 0.001$; ns, not significant.

Results

Decreased CD146 in pulmonary nodules from patients with pulmonary cryptococcosis

Although not specific to pulmonary cryptococcosis, pulmonary nodules are the most common radiological findings [1]. As expected, pulmonary nodules were observed in 10 patients with pulmonary cryptococcosis (Table 1). In contrast to the wide distribution of CD146 in the lung tissues of the healthy tissues, CD146 in the cryptococcus nodules was scarcely expressed (Fig. 1A–C). Collectively, CD146 was significantly decreased in pulmonary nodules with *C. neoformans* pulmonary infection (Fig. 1D), suggesting that CD146 may be involved with pulmonary cryptococcosis.

Pulmonary expression of CD146 was reduced in a mouse model of *C.* pulmonary cryptococcosis

To explore the roles of CD146 in pulmonary cryptococcosis, C57BL/6J mice were infected with the virulent *C. neoformans* strain H99 via intratracheal instillation. The mice were sacrificed at different time points to monitor the fungal burdens and pathological changes. As shown in Fig. 2A, C. *neoformans* H99 led to a progressive increase in lung fungal burdens. As fungi proliferated in the lung, fungemia occurred and subsequently disseminated into the brain (Fig. 2B). Examination of lung tissue stained with H&E revealed markedly increased inflammatory infiltrates during infection (Fig. 2C). Furthermore, PAS staining demonstrated an increase in *C. neoformans* and airway goblet cell metaplasia over time (Fig. 2D). Collectively, we established a mouse model of pulmonary cryptococcosis.

To explore whether CD146 changed during the infection course of pulmonary *C. neoformans*, we quantified CD146 expression with various methods. As shown in Fig. 2E, qRT−PCR revealed that *CD146* mRNA was significantly decreased 3 weeks post infection. Similarly, CD146 protein in lung tissues was significantly reduced in mice 3 weeks following intratracheal infection with *C. neoformans* (Fig. 2F). Furthermore, as observed in the clinical samples, CD146 in the mouse lung *C. neoformans* nodules almost vanished (Fig. 2G). The panoramic distribution of CD146 in the *C. neoformans*-infected lung tissues was diminished in immunofluorescence imaging (Fig. 2H). In summary, as observed in clinical samples, CD146 expression in the mouse model of *C. neoformans* pulmonary infection was decreased.

CD146 deficiency aggravated pulmonary *C. neoformans* infection

To investigate whether CD146 was directly involved in pulmonary cryptococcosis, WT and CD146 KO mice were infected with *C. neoformans* strain H99. Survival curve analysis revealed that CD146 deficiency significantly aggravated pulmonary cryptococcosis (Fig. 3A). In line with the deleterious outcome, fungal burdens in the lung tissues 2 weeks post infection were significantly increased in CD146 KO mice (Fig. 3B). Fungi in the lung tissues disseminated into the spleen and brain. Compared with WT mice, CD146 KO mice displayed a trend toward a higher fungal burden in the spleen (Fig. 3C) and brain (Fig. 3D). Of note, the difference in spleen CFU did not reach statistical significance. Collectively, CD146 deficiency promoted pulmonary *C. neoformans* infection.

CD146 deficiency promoted leukocyte infiltration in pulmonary cryptococcosis

Two weeks post infection, histopathological analysis of lungs with H&E staining revealed increased inflammatory infiltrates around the airways in CD146 KO-infected mice compared with WT controls (Fig. 4A). Similarly, PAS staining demonstrated that goblet cell metaplasia was increased in CD146 KO-infected mice (Fig. 4B). Differential staining

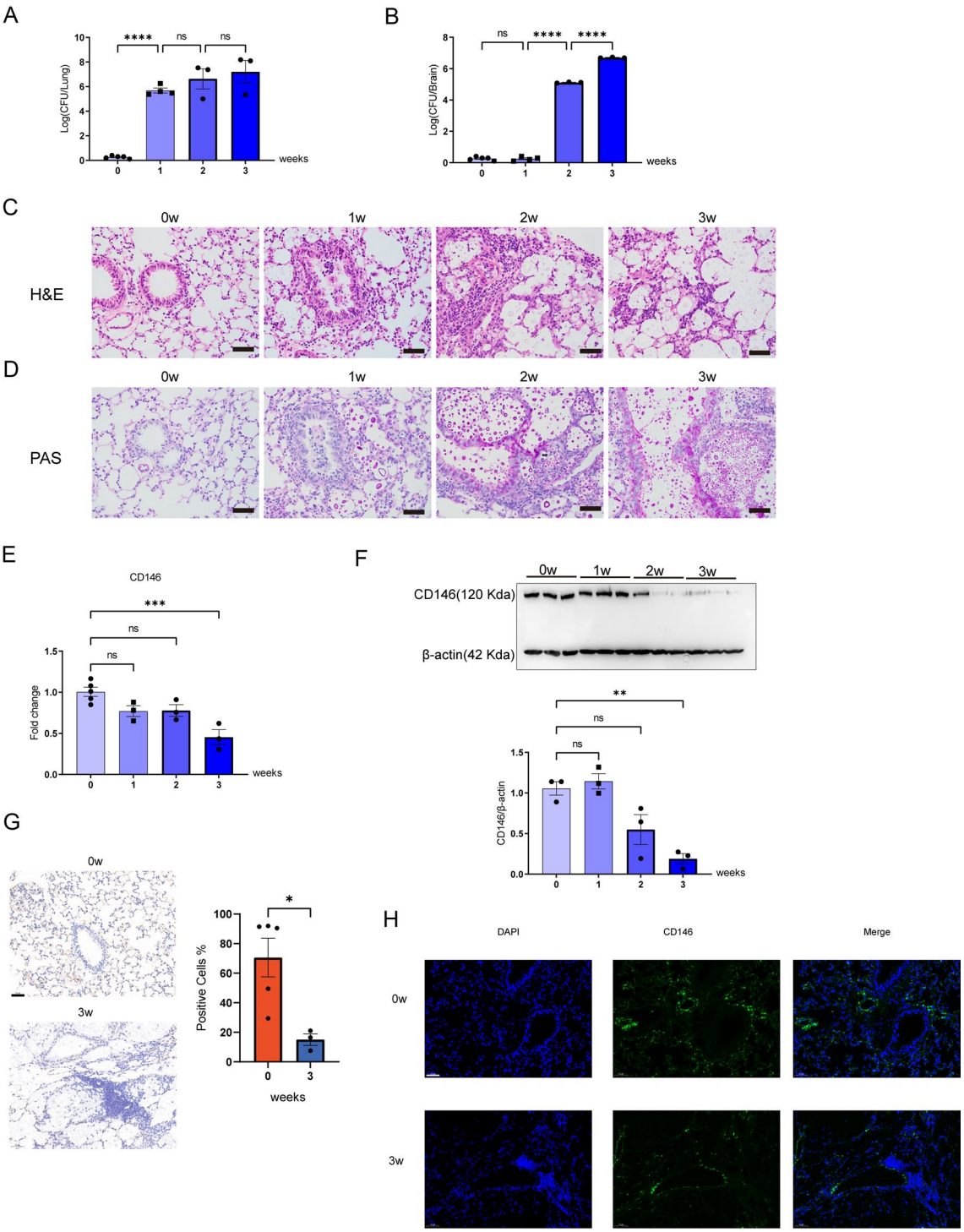

Fig. 2 CD146 was decreased in mice infected with *C. neoformans*. C57BL/6J mice were infected with 10^4 of highly virulent *C. neoformans* strain H99 by intratrachea, and mice were sacrificed at the indicated times. **A**, **B** Lung and brain CFU were enumerated by plating organ homogenates on Sabouraud dextrose agar. **C** Representative lung sections were stained with hematoxylin and eosin stain to analyze the infiltration of inflammatory cells. **D** Representative lung sections were stained with PAS to assess goblet cell hyperplasia. **E**, **F** CD146 in lung tissues was measured by qPCR and Western blotting. The density quantifcation of CD146 was expressed as a ratio relative to β-actin. **G** Immunohistochemical staining for CD146 in lung sections from mice without or with *C. neoformans* infection for 3 weeks. Scale bar 50 μm. **H** Immunofluorescence staining for CD146 in lung sections from mice without or with *C. neoformans* infection for 3 weeks. Scale bar 50 μm. Data were representative of 2 independent experiments with similar results (n = 3–5). *, $p < 0.05$; **, $p < 0.01$; ***, $P < 0.001$; ****, $p < 0.0001$; *ns* not significant

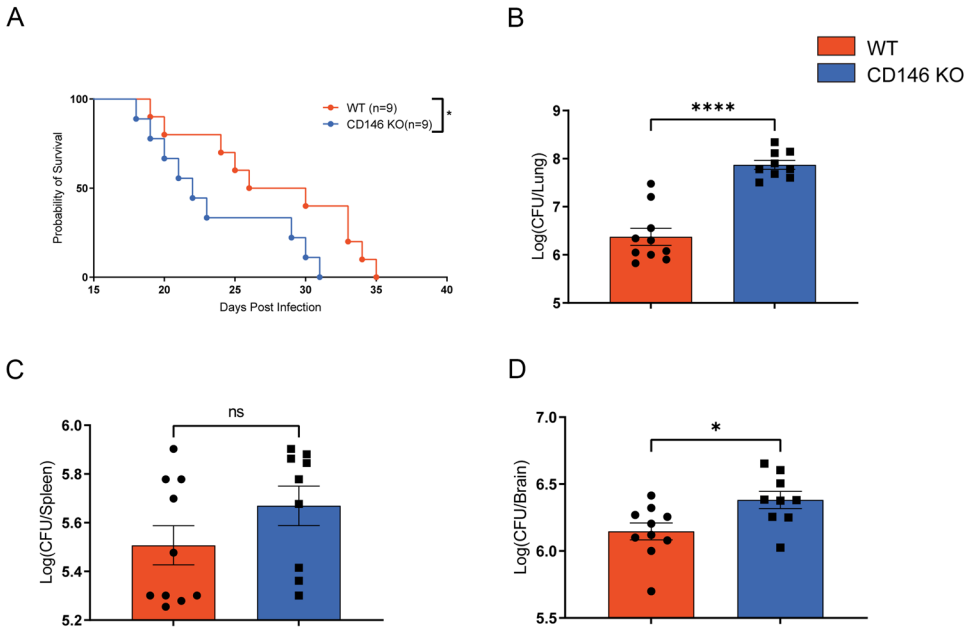

Fig. 3 CD146 deficiency promoted pulmonary *C. neoformans* growth. **A** WT and CD146$^{-/-}$ mice were monitored daily for survival following intratracheal infection with 10^4 CFU *C. neoformans* H99. **B–D** Lung, spleen, and brain CFUs were enumerated 2 weeks post infection by plating organ homogenates on Sabouraud dextrose agar. Data are representative of 2 independent experiments with similar results (n = 9–10). *, $p < 0.05$; ****, $p < 0.0001$; *ns* not significant

of the BAL cells (Figure S1) was completed to determine the pattern of airway inflammation during *C. neoformans* infection. Compared with the airways in WT controls, those of CD146 KO mice presented significant infiltration of leukocytes (neutrophils and macrophages) (Fig. 4C–E). Consistent with these observations, enhanced airway inflammation in CD146 KO mice was associated with the significant upregulation of the keratinocyte-derived chemokine (KC) for neutrophils and monocyte chemoattractant protein-1 (MCP-1) for macrophages (Fig. 4F, G). Thus, in response to *C. neoformans* pulmonary infection, mice deficient in CD146 presented with increased leukocyte recruitment.

To explore whether this increased inflammation in CD146 KO-infected mice was a consequence of CD146 deficiency or simply a reflection of increased fungal burden, we instilled heat-killed fungi (HK-H99) in WT or CD146 KO mice. As shown in Figure S2A-B, the level of TNF-α in lung tissue homogenates from CD146 KO mice was more pronounced than that from their WT counterparts, indicating that CD146 deficiency was at least partially involved in the aggravated pulmonary inflammatory responses.

CD146 deficiency shaped the inflammatory type 2 immune response in *C. neoformans* pulmonary infection

CD4$^+$ T helper (Th) cells are central regulators of anticryptococcal immune responses. Type 2 cytokines are associated with a permissive bronchopulmonary environment for *C. neoformans* growth, whereas type 1-associated cytokines increase fungal killing and elimination [22]. To gain deeper insight into the Th cytokine profile in the absence of CD146 during *C. neoformans* infection, ELISA analysis of BALF (IL-4, IL-5, and IFN-γ) or lung tissue homogenates (TNF-α) was performed. Either type 2 cytokines (IL-4 and IL-5) or type 1 cytokines (IFN-γ and TNF-α) were more pronounced in CD146 KO mice than in their WT counterparts (Fig. 5A–D). However, the ratio of IL-4/IFN-γ was higher in CD146 KO mice (Fig. 5E). We also detected *IL-17A* by qPCR and found that *IL-17A* showed no difference in the pulmonary tissues of CD146 KO-infected mice (Fig. 5F). Collectively, inflammatory type 2 immune responses characterized by elevated IL-4, IL-5, IFN-γ and TNF-α [23] were triggered in CD146$^{-/-}$ mice with *C. neoformans* pulmonary infection.

CD146 in hematopoietic cells was critical for *C. neoformans* infection

Myeloid lineage cells, including macrophages and DCs, are key effector cells against fungi during the first few days after an initial infection [24]. To investigate the cellular basis of the CD146-related antifungal effect in myeloid lineage cells, we generated bone marrow (BM) chimeric mice by reconstituting lethally irradiated WT mice with syngeneic CD146 KO BM or CD146 KO mice with WT BM. As shown in Fig. 6A, compared to WT BM to WT recipient mice, loss of CD146 in hematopoietic cells resulted in increased fungal burdens in lung tissues 2 weeks post infection (WT → WT vs. KO → WT). No difference in the fungal burdens in the lung was found upon the loss of CD146 in nonhematopoietic cells (WT → WT vs. WT → KO). Compared with WT BM to WT recipient mice, CD146 KO BM to WT recipient mice (KO → WT) displayed a higher fungal burden in the spleen

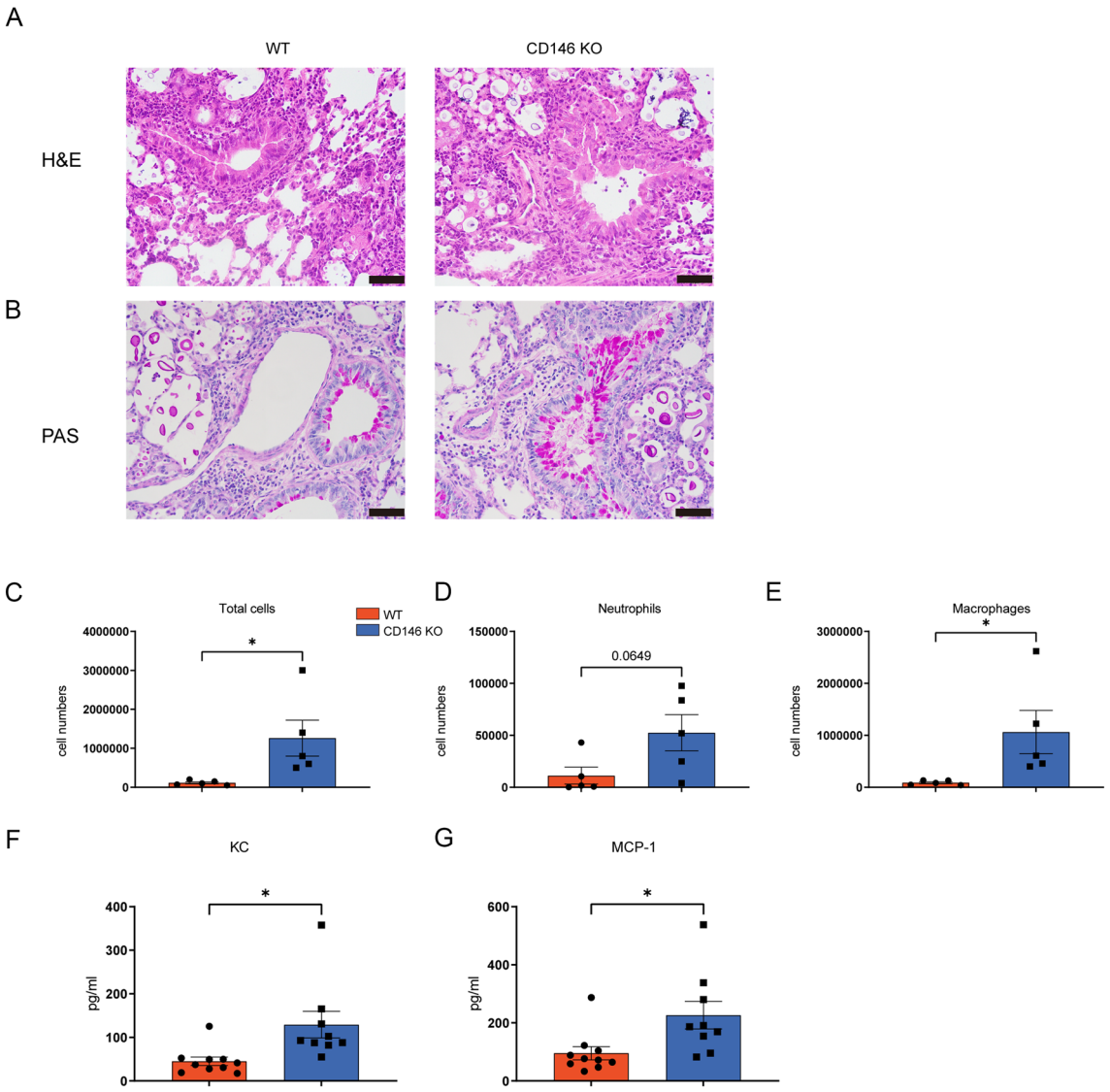

Fig. 4 Increased inflammatory cells in the BALF of CD146$^{-/-}$ mice following cryptococcal infection. At 2 weeks post infection, mice were euthanized and sacrificed for analysis. **A**, **B** Representative lung sections were stained with hematoxylin and eosin stain to analyze the infiltration of inflammatory cells or stained with PAS to assess goblet cell hyperplasia. Scale bar 50 μm. **C**–**E** Numbers of total cells, macrophages, and neutrophils in the BALF of cryptococcal-infected mice. **F**, **G** The concentrations of murine KC and MCP-1 in BALF were determined by ELISA. Data are representative of 2 independent experiments with similar results (n = 9–10). *, $p < 0.05$; *ns* not significant

(Fig. 6B) and brain (Fig. 6C). H&E staining revealed that inflammatory infiltration was significantly increased in lungs where the hematopoietic cells lacked CD146 (Fig. 6D). PAS staining demonstrated that mucus secretion was increased in the airways of the mice that lacked CD146 in their hematopoietic cells (Fig. 6E). The levels of KC and TNF-α were increased in hematopoietic cells or nonhematopoietic cells that lacked CD146 (Fig. 6F, G). In vitro, C. neoformans increased CD146 in macrophages (Fig. 6H), suggesting that CD146 changes in macrophages may be involved in *C. neoformans* infection. Collectively, CD146 deficiency in immune cells (i.e., macrophages) but not in nonimmune cells (i.e., endothelial cells and epithelial cells) was more likely to promote pulmonary *C. neoformans* infection.

CD146 deficiency polarizes M2 macrophages in *C. neoformans* pulmonary infection

Highly induced expression of iNOS is a hallmark of M1, while M2 is marked by expression of Arg1 [15]. In vitro, BMDMs from WT mice infected with H99 (MOI = 10) expressed more *iNOS*. However, the ratio of *Arg1/iNOS* showed no difference (Fig. 7A–C). In the C57BL/6J mice infected with *C. neoformans*, *iNOS* was increased in their

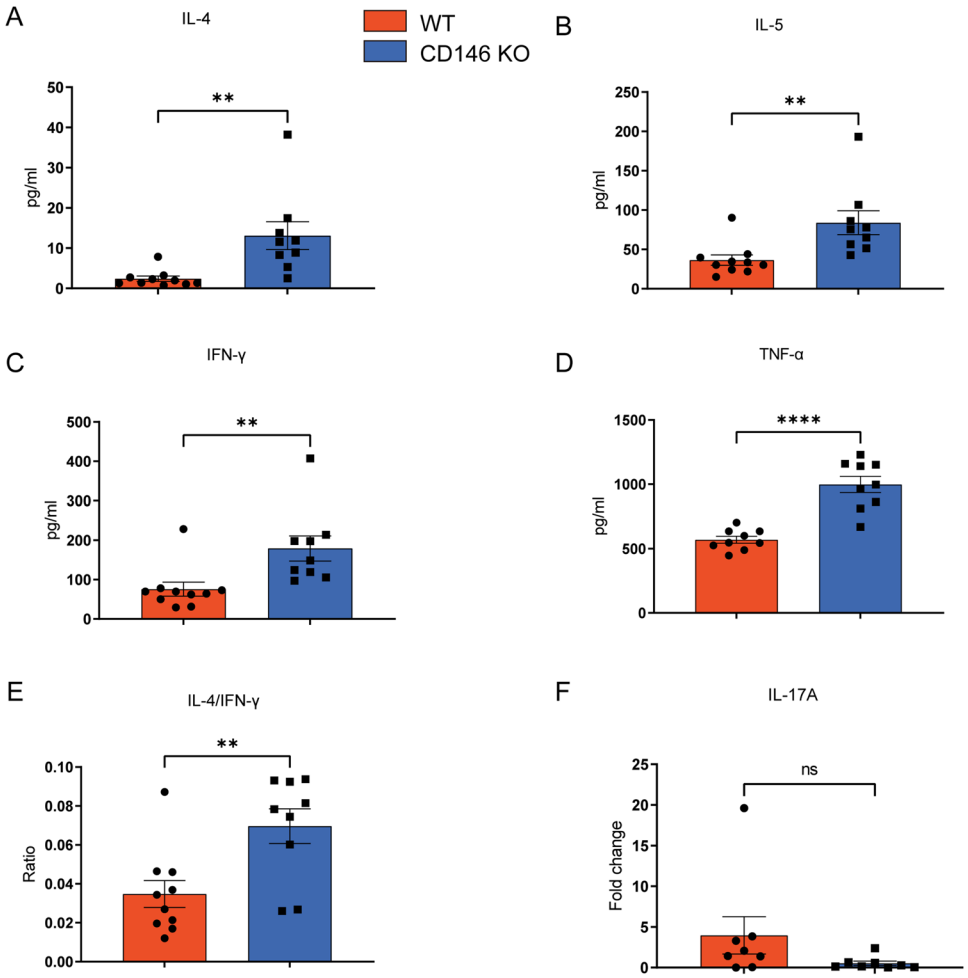

Fig. 5 Pronounced type 2 response in the lungs following cryptococcal infection in CD146$^{-/-}$ mice. At 2 weeks post infection, mice were euthanized and sacrificed for analysis. **A**–**C** IL-4, IL-5, and IFN-γ in BALF were measured with ELISA. **D** TNF-α in the lung homogenates was measured with ELISA. **E** The ratio of IL-4 expression to IFN-γ expression in the two groups. **F** *IL-17*A in the lung homogenates was measured with qPCR. Data are representative of 2 independent experiments with similar results (n = 8–10). **, $p < 0.01$; ****, $p < 0.0001$; *ns* not significant

pulmonary tissues 2 weeks post infection, while *Arg1* was increased 1 week post infection (Fig. 7D–F). However, the pulmonary macrophages were strongly M2-polarized, as the ratio of *Arg1/iNOS* was increased during the infection (Fig. 7G). To further explore the role of CD146 in the polarization of macrophages, we analyzed the mRNA expression of *iNOS* and *Arg1* in lung tissue by RT−qPCR. We found that CD146 deficiency caused a reduction in *iNOS* mRNA at 2 weeks post infection (Fig. 7H). In contrast, *Arg1* mRNA was higher in infected CD146$^{-/-}$ mice (Fig. 7I). Consequently, the pulmonary macrophages were strongly M2-polarized, as the ratio of *Arg1/iNOS* was increased in CD146$^{-/-}$-infected mice (Fig. 7J).

To explore whether the fungi themselves affected the immune responses in the WT and CD146 KO mice, the mRNA levels of *iNOS* and *Arg1* in the lung tissues from the HK-H99-treated mice were also detected. As shown in Figure S2C-D, *Arg1* mRNA was higher in CD146$^{-/-}$-infected mice. The ratio of *Arg1/iNOS* was not statistically significant with the HK-H99 treatments (Figure S2E), suggesting that HK-H99 alone was not sufficient to trigger robust type 2 immune responses. Except for *IL-5*, the mRNA levels of *IL-4*, *IL-13*, *IFN-γ*, *TNF-α*, *iNOS* and *Arg1* showed no difference in the naïve WT and CD146 KO lung tissues (Figure S4A-G). Collectively, CD146 deficiency may promote the polarization of alternatively activated macrophages in pulmonary *C. neoformans* infection.

CD146 deficiency facilitated the production of KC and TNF-α from macrophages after *C. neoformans* infection in vitro

Both TNF-α and KC play critical roles in the recruitment of neutrophils [25]. To investigate the cellular mediators that underlie the different numbers of neutrophils in WT and CD146 KO mice infected with *C. neoformans*, we studied the macrophage responses following in vitro stimulation for 24 h. Differences in macrophage function have been related to susceptibility or resistance to cryptococcal infection [26]. Alveolar macrophages from CD146$^{-/-}$ mice secreted significantly higher levels of KC and TNF-α than those from WT mice (Fig. 8A, B). BMDMs from CD146$^{-/-}$ mice also secreted higher levels of KC and TNF-α under the same conditions (Fig. 8C, D). Taken together, these results indicated

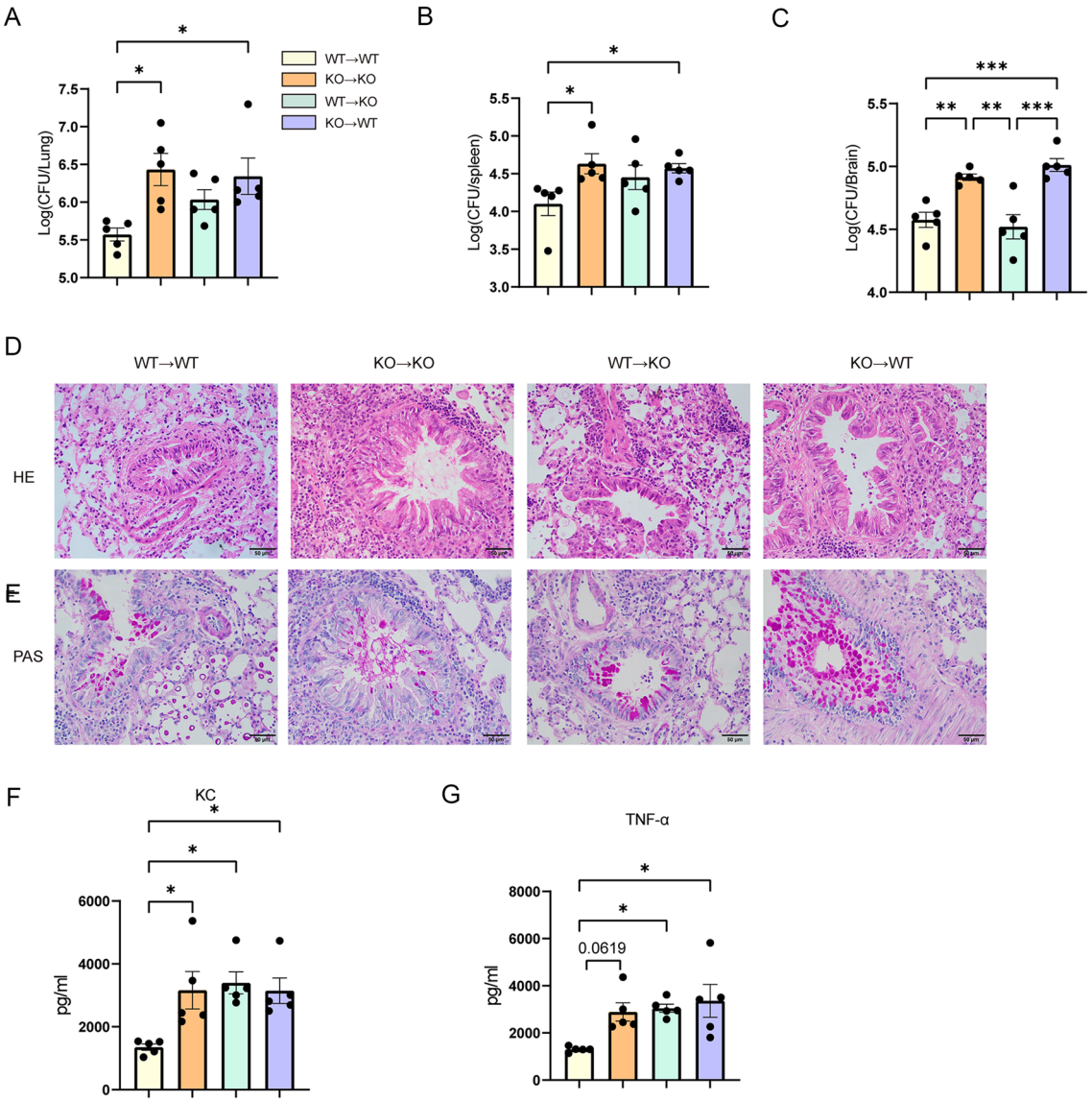

Fig. 6 Loss of CD146 in hematopoietic cells promoted *C. neoformans* infection in vivo. Bone marrow chimeric mice infected with 10^4 *C. neoformans* strain H99 were sacrificed 2 weeks post infection. **A**–**C** Lung, spleen and brain CFUs were enumerated. **D** Representative lung sections were stained with hematoxylin and eosin stain. **E** Representative lung sections were stained with PAS. Scale bar 50 μm. **F**, **G** KC and TNF-α in the lung homogenates were measured with ELISA. *, $p < 0.05$; **, $p < 0.01$; ***, $P < 0.001$; *ns* not significant

that macrophages from CD146 KO mice produced more KC and TNF-α under *C. neoformans* infection, promoting neutrophil infiltration into lung tissues. Alveolar and infiltrating macrophages are able to phagocytize and kill invading pathogens [27]. In our study, however, AMs were not fungicidal. More progressive cryptococcal growth was observed in CD146 KO AMs (Fig. 8E). In contrast, BMDMs from WT or CD146 KO mice were fungicidal; fungal clearance was reduced in CD146 KO BMDMs (Fig. 8F). Reactive oxygen species (ROS) are byproducts of M1 macrophages and are thought to fulfill a critical role in conferring protection against *C. neoformans* infection. As shown in Fig. 8G, H, BMDMs from CD146 KO mice also produced fewer ROS under the same conditions. These results indicated that macrophages from CD146 KO mice were less fungicidal due to the compromised production of ROS.

Discussion

Pulmonary cryptococcosis has diverse clinical manifestations, ranging from asymptomatic infection to possibly fatal pneumonia. Due to limitations in diagnostic tools, pulmonary cryptococcosis is still underdiagnosed [1]. Generally,

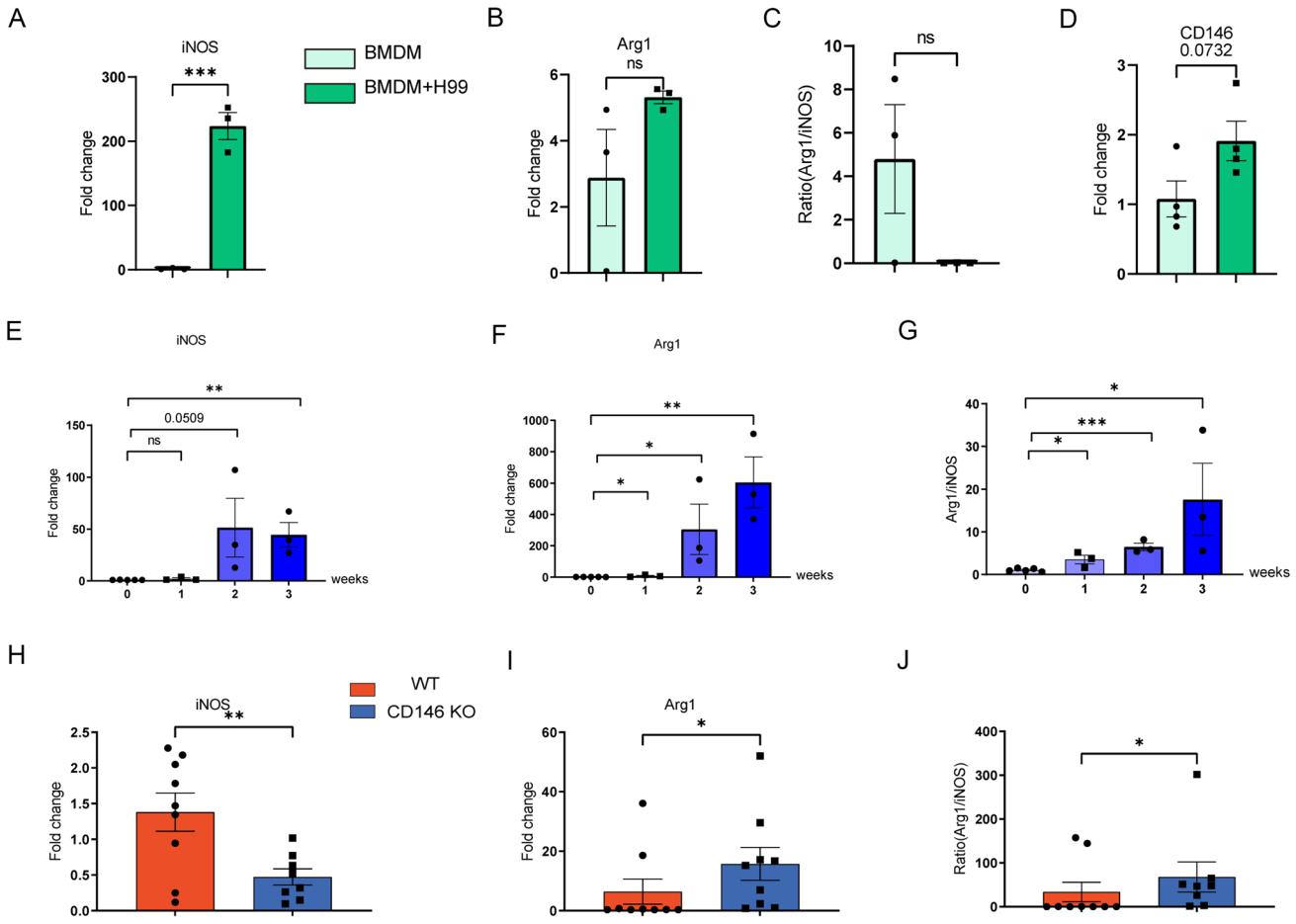

Fig. 7 Increased pulmonary M2 macrophage polarization following cryptococcal infection in CD146$^{-/-}$ mice. **A**–**D** *iNOS*, *Arg1* and *CD146* were examined in BMDMs infected with *C. neoformans* strain H99 (MOI = 10) by qPCR. **E**, **F** Lung mRNA expression levels of the M1 macrophage marker *iNOS* and the M2 macrophage marker *Arg1* at different times of *C. neoformans* H99 infection in C57BL/6J mice. **G** The ratio of *Arg1* expression to *iNOS* expression at different times of *C. neoformans* H99 infection. **H**–**J** Lung mRNA expression levels of the M1 macrophage marker *iNOS* and the M2 macrophage marker *Arg1* in WT and CD146$^{-/-}$ mice 14 days post infection. Data are representative of 2 independent experiments with similar results (n = 5–9). *, $p < 0.05$; **, $p < 0.01$; ***, $P < 0.001$; *ns* not significant

patients with pulmonary cryptococcosis present multiple or solitary nodular opacities. In our clinical samples with *C. neoformans* pulmonary nodules, CD146 expression was significantly diminished in the nodules. In line with the clinical observations, we recorded that pulmonary CD146 expression was significantly decreased in the mice inoculated with *C. neoformans* via intratracheal instillation, suggesting that *C. neoformans* infection may reduce CD146 expression. As a CD146 decrease occurred 3 weeks post infection but not at the early stage, we speculate that the formation of nodules at the later stage of infection may be involved in the decay of CD146 expression.

The second important finding in the present study was that CD146 deficiency aggravated *C. neoformans* infection. CD146 deficiency shortened the survival time and increased the fungal burdens in lung, spleen, and brain tissues. In line with the increased fungal burdens in the lung, type 2 cytokines (IL-4 and IL-5) in the BALF from CD146 KO-infected mice were significantly increased. Unexpectedly, type 1 cytokines (IFN-γ and TNF-α) from CD146$^{-/-}$-infected mice were also increased. As the balance between IL-4 and IFN-γ still shifted in favor of type 2, we concluded that CD146 deficiency promoted inflammatory type 2 immune responses against pulmonary *C. neoformans* infection. Indeed, the infiltration of leukocytes (macrophages and neutrophils) in the lung was increased in CD146$^{-/-}$-infected mice. CD146 deficiency promotes neutrophil and macrophage infiltration [10], which was in line with our observations that CD146 deficiency aggravated lung inflammation in pulmonary cryptococcosis. Of note, the relationships between CD146 and inflammation may be complicated and even contradictory in different diseases. For example, CD146 expression in blood vessels and infiltrated macrophages was positively correlated

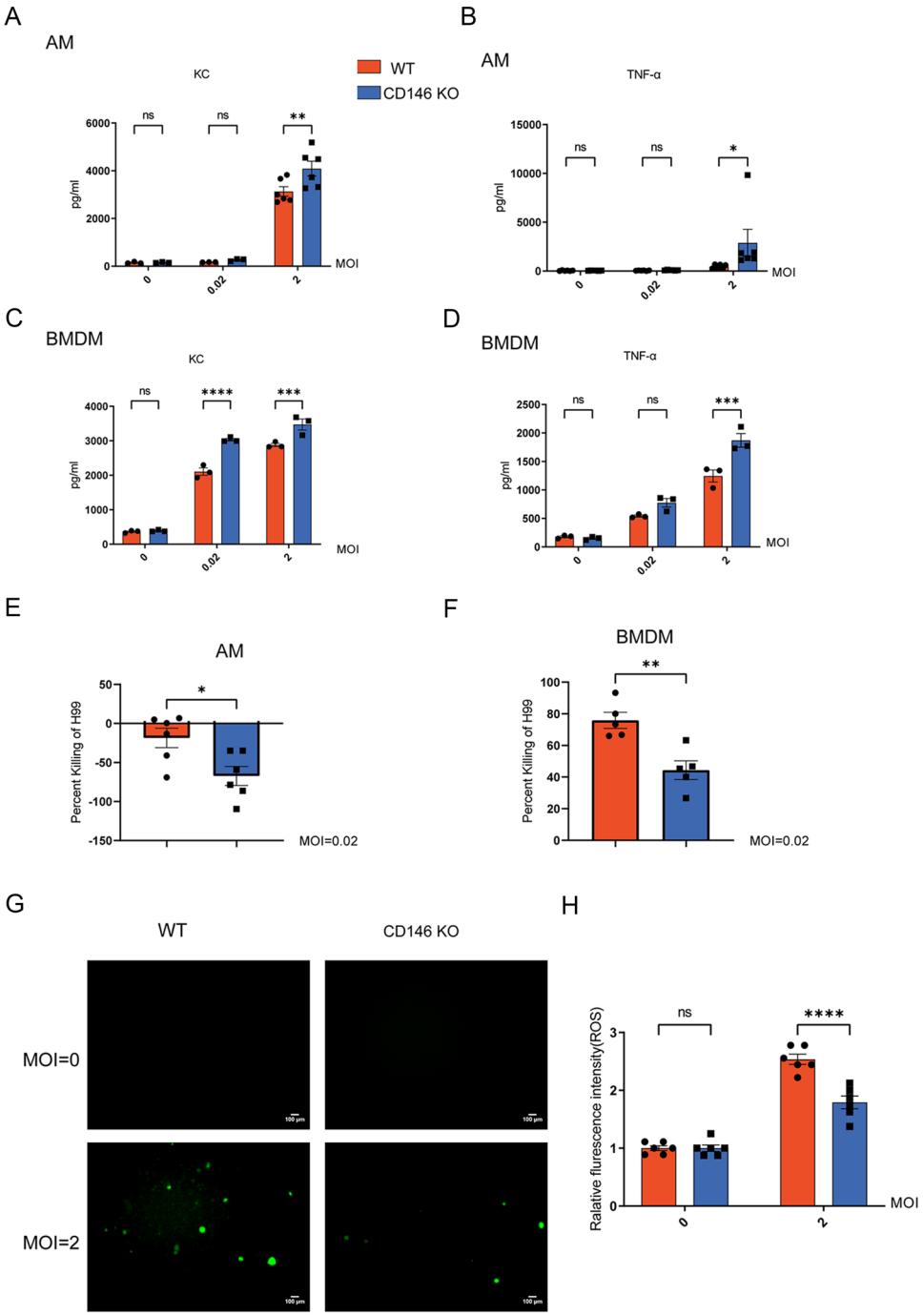

Fig. 8 More KC and TNF-α were produced by CD146$^{-/-}$ macrophages infected with *C. neoformans*. **A**, **B** KC and TNF-α in the supernatant were examined in AMs infected with *C. neoformans* H99 by ELISA. **C**, **D** KC and TNF-α in the supernatant were examined in BMDMs infected with *C. neoformans* strain H99 by ELISA. **E**, **F** Percentage of *C. neoformans* H99 killed by AMs and BMDMs from uninfected WT and CD146$^{-/-}$ mice. **G**, **H** ROS production in BMDMs infected with *C. neoformans* H99 was detected by the DCFH-DA probe with fluorescence microscopy and a microplate reader. Scale bar 100 μm. Data are representative of 2 independent experiments with similar results (n = 3–6). *, $p < 0.05$; **, $p < 0.01$; ***, $P < 0.001$; ****, $p < 0.0001$; *ns* not significant

with inflammation in atherosclerosis [28]. Moreover, CD146 deficiency reduced the adhesion of *C. neoformans* to the epithelium and decreased the fungal burden in a 4-h acute infection model [13]. In contrast, CD146 deficiency promoted inflammatory type 2 immune responses and exaggerated pulmonary *C. neoformans* infection in a 2–3 week chronic infection model. Considering that CD146 is expressed by epithelial cells, macrophages, and other cells, we speculated that CD146 in different cells may play diverse roles in different diseases.

Alternatively, activated macrophages (M2) were permissive niches for *C. neoformans* infection. Another finding in the present study was that CD146 deficiency promoted macrophage activation and M2 macrophage polarization. CD146-deficient macrophages produced more KC and TNF-α, which may promote leukocyte recruitment in mice following C. neoformans infection. Alveolar macrophages (AMs) and bone marrow-derived macrophages (BMDMs) are different. AMs reside in lung tissues. BMDMs reflect infiltrating macrophages from

blood into lung tissues upon infection. Depletion of AM decreased *C. neoformans* pulmonary infection [29], suggesting that AMs may be accomplices in *C. neoformans* survival. Accordingly, $CD146^{-/-}$ AM boosted *C. neoformans* proliferation. The roles of BMDMs in *C. neoformans* pulmonary infection are more complicated [30]. At the early stage, infiltrated macrophages may help control the infection [31]. $CD146^{-/-}$ BMDMs were less fungicidal and produced fewer ROS, which was in accordance with the increased fungal burdens in $CD146^{-/-}$-infected mice. Macrophages originate from hematopoietic cells. Observations from chimeric mouse experiments indicated that CD146 deficiency in hematopoietic cells but not in nonhematopoietic cells was more likely to aggravate pulmonary *C. neoformans* infection, suggesting that CD146 deficiency in macrophages may be involved in pulmonary cryptococcosis. As demonstrated, CD146 deficiency impaired the killing ability of BMDMs but increased the proliferation of fungi in AMs. Therefore, CD146 deficiency may indirectly promote M2 differentiation in vivo by increasing the fungal burden in the lung.

Our study is not without limitations. First, the sample size of clinical tissues was small, which may weaken the clinical significance of CD146 in pulmonary *C. neoformans* infection. CD146 expression is closely associated with cancers [32], kidney transplantation [33], systemic sclerosis [34] and other diseases [35]. More samples are required to address the clinical significance of CD146 in pulmonary *C. neoformans* infection. Second, the killing ability of macrophages overexpressing CD146 remains to be elucidated, which would improve our understanding of CD146 in the regulation of macrophages. CD146 deficiency boosted the production of TNF-α in macrophages stimulated with *C. neoformans*. The mechanism analysis warrants further investigation. Third, in our flow cytometry, we determined macrophages as $CD45^{+}F4/80^{+}$. However, several studies have reported that F4/80 is also expressed in lung $CD11b^{+}$ dendritic cells [36] and eosinophils [37]. More markers to distinguish macrophages and other cells in the type 2 immunity of pulmonary cryptococcosis are needed.

In summary, we demonstrated that CD146 expression was decreased in pulmonary cryptococcosis clinical samples and in mice following intratracheal inoculation with *C. neoformans*. CD146 deficiency shaped inflammatory type 2 immune responses, which favored the survival of fungi and exaggerated pulmonary infection. Macrophages defective with CD146 produced more KC and TNF-α, which further recruited more neutrophils and macrophages in mice following *C. neoformans* challenge. CD146 deficiency in hematopoietic cells was vital for this process. Further studies aiming to improve CD146 expression may help to conquer pulmonary cryptococcosis.

Supplementary Information The online version contains supplementary material available at https://doi.org/10.1007/s00430-023-00780-x.

Author contributions Conceptualization, XY, MH, YB, NJ, and MZ; formal analysis, ZW, WL, JJ, and MZ; funding acquisition, YB and MZ; investigation, WL and HH; methodology, ZW, WL, HH, JJ, CY, XZ, QY, and XY; project administration, MZ; resources, HH and YB; supervision, MZ; validation, ZW; writing—original draft, ZW; writing—review and editing, YB, NJ, and MZ.

Funding This research was supported by the National Natural Science Foundation of China (82171738, 81671563), the Jiangsu Provincial Commission of Health and Family Planning (Q2017001), and the Shenzhen Science and Technology Program (JCYJ20210324115607021).

Data availability The datasets used and/or analyzed during the present study are available from the corresponding author on reasonable request.

Declarations

Conflict of interest The authors have no conflicts of interest to declare.

References

1. Setianingrum F, Rautemaa-Richardson R, Denning DW (2019) Pulmonary cryptococcosis: a review of pathobiology and clinical aspects. Med Mycol 57(2):133–150
2. Davis MJ, Tsang TM, Qiu Y, Dayrit JK, Freij JB, Huffnagle GB et al (2013) Macrophage M1/M2 polarization dynamically adapts to changes in cytokine microenvironments in Cryptococcus neoformans infection. MBio 4(3):e00264-e313
3. Deerhake ME, Reyes EY, Xu-Vanpala S, Shinohara ML (2021) Single-cell transcriptional heterogeneity of neutrophils during acute pulmonary *Cryptococcus neoformans* infection. Front Immunol 12:670574
4. Sun D, Zhang M, Liu G, Wu H, Zhu X, Zhou H et al (2016) Real-time imaging of interactions of neutrophils with *Cryptococcus neoformans* demonstrates a crucial role of complement C5a–C5aR signaling. Infect Immun 84(1):216–229
5. Mednick AJ, Feldmesser M, Rivera J, Casadevall A (2003) Neutropenia alters lung cytokine production in mice and reduces their susceptibility to pulmonary cryptococcosis. Eur J Immunol 33(6):1744–1753
6. Sun Z, Ji N, Jiang J, Tao Y, Zhang E, Yang X et al (2020) Fine particulate matter (PM2.5) promotes CD146 expression in alveolar epithelial cells and *Cryptococcus neoformans* pulmonary infection. Front Microbiol 11:525976
7. Wang Z, Yan X (2013) CD146, a multifunctional molecule beyond adhesion. Cancer Lett 330(2):150–162
8. Bardin N, Blot-Chabaud M, Despoix N, Kebir A, Harhouri K, Arsanto JP et al (2009) CD146 and its soluble form regulate monocyte transendothelial migration. Arterioscler Thromb Vasc Biol 29(5):746–753
9. Luo Y, Duan H, Qian Y, Feng L, Wu Z, Wang F et al (2017) Macrophagic CD146 promotes foam cell formation and retention during atherosclerosis. Cell Res 27(3):352–372
10. Blin MG, Bachelier R, Fallague K, Moussouni K, Aurrand-Lions M, Fernandez S et al (2019) CD146 deficiency promotes plaque formation in a mouse model of atherosclerosis by enhancing RANTES secretion and leukocyte recruitment. J Mol Cell Cardiol 130:76–87

11. Duan H, Jing L, Xiang J, Ju C, Wu Z, Liu J et al (2022) CD146 associates with Gp130 to control a macrophage pro-inflammatory program that regulates the metabolic response to obesity. Adv Sci (Weinh) 9(13):e2103719
12. Zhang B, Li L, Feng L, Zhang Y, Zeng X, Feng J et al (2009) Elevated levels of soluble and neutrophil CD146 in active systemic vasculitis. Lab Med 40(6):351–356
13. Sun Z, Ji N, Jiang J, Tao Y, Zhang E, Yang X et al (2020) Fine particulate matter (PM(2).(5)) promotes CD146 expression in alveolar epithelial cells and *Cryptococcus neoformans* pulmonary infection. Front Microbiol 11:525976
14. Surawut S, Ondee T, Taratummarat S, Palaga T, Pisitkun P, Chindamporn A et al (2017) The role of macrophages in the susceptibility of Fc gamma receptor IIb deficient mice to *Cryptococcus neoformans*. Sci Rep 7:40006
15. Flaczyk A, Duerr CU, Shourian M, Lafferty EI, Fritz JH, Qureshi ST (2013) IL-33 signaling regulates innate and adaptive immunity to *Cryptococcus neoformans*. J Immunol 191(5):2503–2513
16. Benonisson H, Altıntaş I, Sluijter M, Verploegen S, Labrijn AF, Schuurhuis DH et al (2019) CD3-bispecific antibody therapy turns solid tumors into inflammatory sites but does not install protective memory. Mol Cancer Ther 18(2):312–322
17. Dai X, Mao C, Lan X, Chen H, Li M, Bai J et al (2017) Acute *Penicillium marneffei* infection stimulates host M1/M2a macrophages polarization in BALB/C mice. BMC Microbiol 17(1):177
18. Liu Y, Yuan Q, Zhang X, Chen Z, Jia X, Wang M et al (2023) Fine particulate matter (PM2.5) induces inhibitory memory alveolar macrophages through the AhR/IL-33 pathway. Cell Immunol 386:104694
19. Osterholzer JJ, Chen GH, Olszewski MA, Zhang YM, Curtis JL, Huffnagle GB et al (2011) Chemokine receptor 2-mediated accumulation of fungicidal exudate macrophages in mice that clear cryptococcal lung infection. Am J Pathol 178(1):198–211
20. Huang HR, Li F, Han H, Xu X, Li N, Wang S et al (2018) Dectin-3 recognizes glucuronoxylomannan of *Cryptococcus neoformans* serotype AD and *Cryptococcus gattii* serotype B to initiate host defense against cryptococcosis. Front Immunol 9:1781
21. Nakamura Y, Sato K, Yamamoto H, Matsumura K, Matsumoto I, Nomura T et al (2015) Dectin-2 deficiency promotes Th2 response and mucin production in the lungs after pulmonary infection with *Cryptococcus neoformans*. Infect Immun 83(2):671–681
22. Piehler D, Stenzel W, Grahnert A, Held J, Richter L, Kohler G et al (2011) Eosinophils contribute to IL-4 production and shape the T-helper cytokine profile and inflammatory response in pulmonary cryptococcosis. Am J Pathol 179(2):733–744
23. Lloyd CM, Snelgrove RJ (2018) Type 2 immunity: expanding our view. Sci Immunol 3(25):eaat1604
24. Zhao X, Guo Y, Jiang C, Chang Q, Zhang S, Luo T et al (2017) JNK1 negatively controls antifungal innate immunity by suppressing CD23 expression. Nat Med 23(3):337–346
25. Ishizuka S, Yokoyama R, Sato K, Shiroma R, Nakahira A, Yamamoto H et al (2020) Effect of CARD9 deficiency on neutrophil-mediated host defense against pulmonary infection with *Streptococcus pneumoniae*. Infect Immun 89(1):e00305-e320
26. Guillot L, Carroll SF, Homer R, Qureshi ST (2008) Enhanced innate immune responsiveness to pulmonary *Cryptococcus neoformans* infection is associated with resistance to progressive infection. Infect Immun 76(10):4745–4756
27. Leopold Wager CM, Wormley FL Jr (2014) Classical versus alternative macrophage activation: the Ying and the Yang in host defense against pulmonary fungal infections. Mucosal Immunol 7(5):1023–1035
28. Qian YN, Luo YT, Duan HX, Feng LQ, Bi Q, Wang YJ et al (2014) Adhesion molecule CD146 and its soluble form correlate well with carotid atherosclerosis and plaque instability. CNS Neurosci Ther 20(5):438–445
29. Kechichian TB, Shea J, Del Poeta M (2007) Depletion of alveolar macrophages decreases the dissemination of a glucosylceramide-deficient mutant of *Cryptococcus neoformans* in immunodeficient mice. Infect Immun 75(10):4792–4798
30. Nelson BN, Daugherty CS, Sharp RR, Booth JL, Patel VI, Metcalf JP et al (2022) Protective interaction of human phagocytic APC subsets with *Cryptococcus neoformans* induces genes associated with metabolism and antigen presentation. Front Immunol 13:1054477
31. Coelho C, Souza AC, Derengowski Lda S, de Leon-Rodriguez C, Wang B, Leon-Rivera R et al (2015) Macrophage mitochondrial and stress response to ingestion of *Cryptococcus neoformans*. J Immunol 194(5):2345–2357
32. de Kruijff IE, Timmermans AM, den Bakker MA, Trapman-Jansen A, Foekens R, Meijer-Van Gelder ME et al (2018) The prevalence of CD146 expression in breast cancer subtypes and its relation to outcome. Cancers (Basel) 10(5):134
33. Liao J, Fu Q, Chen W, Li J, Zhang W, Zhang H et al (2020) Plasma soluble CD146 as a potential diagnostic marker of acute rejection in kidney transplantation. Front Med (Lausanne) 7:531999
34. Ito T, Tamura N, Okuda S, Tada K, Matsushita M, Yamaji K et al (2017) Elevated serum levels of soluble CD146 in patients with systemic sclerosis. Clin Rheumatol 36(1):119–124
35. Sun Z, Ji N, Ma Q, Zhu R, Chen Z, Wang Z et al (2020) Epithelial-mesenchymal transition in asthma airway remodeling is regulated by the IL-33/CD146 axis. Front Immunol 11:1598
36. Misharin AV, Morales-Nebreda L, Mutlu GM, Budinger GR, Perlman H (2013) Flow cytometric analysis of macrophages and dendritic cell subsets in the mouse lung. Am J Respir Cell Mol Biol 49(4):503–510
37. Rose CE Jr, Lannigan JA, Kim P, Lee JJ, Fu SM, Sung SS (2010) Murine lung eosinophil activation and chemokine production in allergic airway inflammation. Cell Mol Immunol 7(5):361–374